Lipid mediators in innate immunity against tuberculosis: opposing roles of PGE$_2$ and LXA$_4$ in the induction of macrophage death

Minjian Chen,[1] Maziar Divangahi,[1] Huixian Gan,[1] Daniel S.J. Shin,[1] Song Hong,[2] David M. Lee,[1] Charles N. Serhan,[2] Samuel M. Behar,[1] and Heinz G. Remold[1]

[1]Department of Medicine and Division of Rheumatology, Immunology, and Allergy and [2]Center for Experimental Therapeutics and Reperfusion Injury, Department of Anesthesiology, Perioperative, and Pain Medicine, Brigham and Women's Hospital and Harvard Medical School, Boston, MA 02115

Virulent *Mycobacterium tuberculosis* (*Mtb*) induces a maladaptive cytolytic death modality, necrosis, which is advantageous for the pathogen. We report that necrosis of macrophages infected with the virulent *Mtb* strains H37Rv and Erdmann depends on predominant LXA$_4$ production that is part of the antiinflammatory and inflammation–resolving action induced by *Mtb*. Infection of macrophages with the avirulent H37Ra triggers production of high levels of the prostanoid PGE$_2$, which promotes protection against mitochondrial inner membrane perturbation and necrosis. In contrast to H37Ra infection, PGE$_2$ production is significantly reduced in H37Rv–infected macrophages. PGE$_2$ acts by engaging the PGE$_2$ receptor EP2, which induces cyclic AMP production and protein kinase A activation. To verify a role for PGE$_2$ in control of bacterial growth, we show that infection of prostaglandin E synthase (PGES)$^{-/-}$ macrophages in vitro with H37Rv resulted in significantly higher bacterial burden compared with wild–type macrophages. More importantly, PGES$^{-/-}$ mice harbor significantly higher *Mtb* lung burden 5 wk after low–dose aerosol infection with virulent *Mtb*. These in vitro and in vivo data indicate that PGE$_2$ plays a critical role in inhibition of *Mtb* replication.

CORRESPONDENCE
Heinz G. Remold:
hremold@rics.bwh.harvard.edu

Abbreviations used: 5-LO, 5-lipoxygenase; AA, arachidonic acid; COX, cyclooxygenase; cPLA$_2$, cytosolic PLA$_2$; EP, E prostanoid; LC-MS-MS, liquid chromatography tandem mass spectrometry; MOI, multiplicity of infection; mPGES, microsomal prostaglandin E synthase; MPT, mitochondrial permeability transition; PI, propidium iodide; PI3K, phosphatidylinositol-3 kinase; PKA, protein kinase A; siRNA, small interfering RNA.

Tuberculosis is the predominant cause for mortality from chronic pulmonary bacterial infections worldwide causing nearly two million deaths yearly. Tuberculosis has become more serious as a consequence of the global AIDS epidemic and the emergence of multidrug-resistant *Mycobacterium tuberculosis* (*Mtb*), the causative agent of tuberculosis (1). Natural transmission of *Mtb* occurs predominantly via inhalation of aerosols containing small numbers of bacteria that are deposited in the distal airways of the lung (2). The pathogens are phagocytosed by pulmonary Mφ, which serve as a sanctuary for *Mtb* (3). Virulent *Mtb*, which

reside in Mφ, initially evade elimination by the immune system via preventing apoptosis and inhibiting maturation of the phagosome–lysosome organelle of the host Mφ (4, 5). The net effect is to diminish entry of bacterial proteins into the class II MHC antigen-processing pathway (4) and to create a protected intracellular milieu where bacilli remain metabolically active and replication competent (6). For Mφ infected with virulent H37Rv, necrosis characterized by cytolysis is the dominant form of cell death, which affords a protective milieu for *Mtb* (7, 8). Thus, subversion of cell death toward necrosis is of considerable advantage for the pathogen.

A common mechanism of necrosis is induction of mitochondrial permeability transition (MPT), which is manifested as accelerated cell death with plasma membrane disintegration. It is thought that a pore opens in the inner mitochondrial membrane allowing water and other molecules to pass through. Opening of this permeability transition pore can be triggered by multiple stimuli and leads to dissipation of the mitochondrial inner membrane potential ($\Delta\Psi_m$) (9). Irreversible induction of MPT leads to mitochondrial damage associated with mitochondrial swelling and subsequent necrosis of the cell. In vitro Mφ infected with virulent H37Rv causes the catastrophic irreversible MPT that commits the Mφ to necrosis (10).

The active nature of this necrosis induction by virulent *Mtb* is clearly revealed after infection of Mφ with mutants of *Mtb*. Although host Mφ support growth of virulent *Mtb* (3), innate immune mechanisms are activated that limit pathogen survival after infection with *Mtb* mutants having altered virulence. These responses include induction of apoptosis, a slow cell death modality which leaves the plasma membrane intact and is observed after infection of Mφ with attenuated *Mtb* (11–13). This Mφ death modality limits exploitation of the intracellular growth environment through direct microbicidal effects and by sequestering bacilli in apoptotic bodies. Indeed, apoptosis both enhances antigen presentation by DC (14) and facilitates efficient pathogen killing (15–18).

Two pathways are described that lead to this highly regulated form of cell death (19). First, the extrinsic apoptotic pathway implicates binding of the ligands TNF and FasL to their receptors that trigger apoptosis (20). Second, the intrinsic apoptotic pathway involves the mitochondria, which release cytochrome *c* and other factors from the mitochondrial intermembrane space that promote apoptosis (21, 22).

We demonstrated previously that mitochondria play an essential role to determine whether *Mtb*-infected Mφ undergo cytolytic necrosis or apoptosis (8). Apoptosis induced by the mitochondrial pathway commences with Ca^{2+} release from the ER that leads to an increase of Ca^{2+} in the mitochondria as well as translocation of BAX into the mitochondria and BAK activation (23). Permeabilization of the mitochondrial outer membrane then proceeds via formation of a proteolipid pore and subsequent escape of proteins from the mitochondrial intermembrane space into the cytosol. More specifically, upon mitochondrial outer membrane permeabilization proapoptotic factors, including cytochrome *c*, are released from the mitochondrial intermembrane space into the cytosol. There, cytochrome *c* forms a complex with Apaf-1, leading to activation of caspase-9 that, in turn, activates executioner caspases such as caspase-3, -6, and -7, which are instrumental in the induction of apoptosis (19, 24).

Infection with the attenuated *Mtb* H37Ra, which has a mutation in PhoP which inhibits ESX-1 function (25), predominantly prevents necrosis and leads to sequestration and decimation of the intracellular bacteria (8, 26).

Mtb-induced apoptosis and antimycobacterial activity of human Mφ requires the activity of cPLA$_2$-γ, a group IV cytosolic PLA$_2$ (cPLA$_2$) (27) which catalyzes the release of arachidonic acid (AA) from the sn-2 position of membrane phospholipids (28). AA and its functionally diverse and biologically active eicosanoid products have been implicated in the regulation of programmed cell death in several cell types (29, 30). The lipoxins are AA metabolites generated by 5- and 15-lipoxygenases (5- and 15-LO) (31). Lipoxins modulate chemokine and cytokine expression, stimulate monocyte trafficking, and enhance Mφ engulfment of apoptotic leucocytes (32). However the role of 5-LO products of AA such as lipoxins and leukotriene B$_4$, which amplifies PMN chemotaxis and production of granule products (33), has not been elucidated in modulating the death modality of Mφ.

Prostanoids are lipid mediators generated from AA by the enzymatic action of the cyclooxygenases (COX) 1 and 2 to form the intermediate PGH$_2$, with subsequent metabolism to specific prostanoid species (e.g., PGD$_2$, PGE$_2$, PGF$_{2\alpha}$, PGI$_2$, and thromboxane) by prostaglandin synthases (34, 35). The functions of these prostanoids are defined by an array of specific receptors. In the case of PGE$_2$, differential expression of four distinct EP receptors defines the intracellular pathways that are activated by PGE$_2$ and results in specific functions that might either promote or inhibit inflammation. For example, in the lung, PGE$_2$ either promotes vasodilatation and increases vascular permeability or increases bronchodilatation (36). A recent study describes a noninflammatory function of PGE$_2$, up- or down-regulation of programmed cell death, which indicates that the mechanisms of PGE$_2$ activation are complex and context dependent (37).

Mice with a deleted 5-LO gene have increased IL-12, IFN-γ, and NO synthase 2 levels compared with WT mice after pulmonary *Mtb* infection. 5-LO$^{-/-}$ mice also have significantly lower *Mtb* burdens and survive longer than WT animals after respiratory *Mtb* infection (38). Importantly, administration of a stable LXA$_4$ analogue was sufficient to reverse the increased resistance of 5-LO$^{-/-}$ mice to *Mtb* infection. The finding that *Mtb* infection significantly increases AA production via activation of cPLA$_2$-γ (27) and that 5 LO$^{-/-}$ mice are significantly more resistant to *Mtb* infections (38), raised the question of whether eicosanoid production is involved in macrophage necrosis and inhibition of apoptosis induced by virulent *Mtb*. We hypothesize that stimulation of lipoxin by virulent *Mtb* inhibits macrophage apoptosis, promotes necrosis, and represents a mechanism that allows *Mtb* to evade elimination by the innate immune system. We therefore investigated how lipoxins and prostanoids affect the outcome of *Mtb*-driven Mφ death with respect to apoptosis and necrosis as a novel pathogenic mechanism that regulates the innate immune response in *Mtb* infection.

RESULTS

Virulent *Mtb* trigger production of LXA$_4$ in Mφ

We demonstrated that inhibition of cPLA$_2$ abrogates apoptosis in *Mtb*-infected Mφ, which could be restored by reconstitution of AA, the predominant product of cPLA$_2$ (27). These findings suggest that products synthesized from AA, namely the eicosanoids, regulate programmed Mφ death induced

by *Mtb*. Two groups of eicosanoids are of special interest because of their opposing effects, the prostanoids that are derived by the COX pathway (34) and the lipoxins, a distinct class of LO-derived products which promote termination of inflammation (39).

The identification of PGE_2 and LXA_4 in infected Mφ supernatants was established from the diagnostic ions present in their liquid chromatography tandem mass spectrometry (LC-MS-MS) spectra (Fig. 1 A). We extended these studies by performing ELISA assays on H37Rv- and H37Ra-infected Mφ.
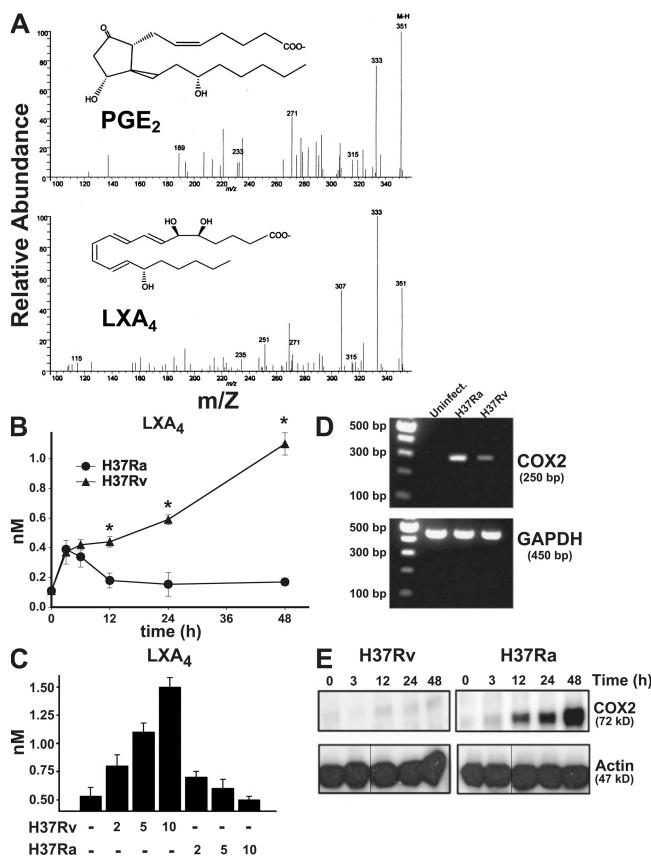
Figure 1. LXA_4 and COX2 production of human Mφ infected with H37Rv and H37Ra. (A) LC-MS-MS of endogenous PGE_2 (top) and LXA_4 (bottom) produced by H37Ra- (MOI 10) and H37Rv- (MOI 10) infected human Mφ, respectively, at 24 h. The spectrum is a representative LC-MS-MS ($n = 3$). The prominent ions and relative intensity matched with authentic PGE_2 and LXA_4 under these LC-MS-MS conditions. (B) LXA_4 production in human Mφ infected with H37Rv and H37Ra (MOI 10:1) at 0–48 h. Differences in LXA_4 concentrations in supernatants from H37Ra- and H37Rv-infected Mφ are statistically significant (*, $P < 0.002$; $n = 3$). (C) LXA_4 accumulation at 48 h in Mφ supernatants infected with H37Ra and H37Rv (MOI 2, 5, and 10:1). The differences in LXA_4 production induced by H37Ra and H37Rv are statistically significant at all MOIs ($P < 0.01$; $n = 3$). (D) COX2 mRNA accumulation in Mφ infected with H37Ra or H37Rv (MOI 10:1; uninfect, uninfected). (E) Production of COX2 protein in Mφ infected with H37Ra and H37Rv (MOI 10:1) at different time points. In all studies, n represents the number of independent experiments and the error bars represent SE. Black lines indicate that intervening lanes have been spliced out.

The production of LXA_4 was measured over time in supernatants from Mφ infected with virulent and avirulent *Mtb*. Virulent H37Rv induce significantly higher levels of LXA_4 production (1 nM; Fig. 1 B). Similar results are observed with another virulent strain (Erdmann strain [not depicted]). In contrast, when Mφ are infected with avirulent H37Ra, production of LXA_4 reaches ∼0.4 nM at 4 and 6 h after infection but is then subsequently down-regulated to ∼0.2 nM at 12 h. The amount of LXA_4 production induced by H37Rv correlates with the multiplicity of infection (MOI; Fig. 1 C). In contrast, the amount of LXA_4 production after H37Ra infection was not increased when the MOI was raised.

These findings raised the question of whether Mφ infected with virulent *Mtb* negatively regulate COX2 expression. Infection of Mφ with the virulent H37Rv induced little accumulation of COX2 mRNA and COX2 protein compared with infection with the mutant *Mtb* strain H37Ra, suggesting that H37Rv infection inhibits COX2 expression (Fig. 1, D and E). These findings suggest that infection with virulent *Mtb* induces the production of LXA_4 in sufficient quantities to inhibit COX2 production, which represents an important manifestation of bacterial virulence.

The virulent *Mtb* strain H37Rv inhibits prostanoid production by the host Mφ

COX2, the inducible PGH synthase, is required for prostanoid synthesis (40). To study whether inhibition of COX2 expression by H37Rv had any functional consequences, we measured prostanoid production by *Mtb*-infected Mφ. PGE_2 levels of <1 nM were detected in supernatants of H37Rv-infected Mφ during the first 48 h of infection. In contrast, levels of PGE_2 were produced by Mφ infected with H37Ra, which increased over time and could be correlated with the MOI (Fig. 2, A and B). Infection with H37Ra also significantly induced production of the prostanoids $PGF_{2\alpha}$ (Fig. 2 C) and TXA_2 (not depicted). In contrast, the virulent *Mtb* strain H37Rv failed to induce significant prostanoid production (Fig. 2, A–C). To determine whether these findings were not confounded by altered bacterial uptake, survival, or replication, we measured bacterial counts. 72 h after infection, the bacterial burden was similar between Mφ infected with H37Rv and H37Ra (unpublished data).

Thus, virulent *Mtb* suppress COX2 expression in infected Mφ, which leads to a global inhibition of prostanoid production. Although prostanoid synthesis is significantly inhibited by H37Rv, the amount that is produced is likely to be an important counterbalance to LXA_4 because Mφ exposed to 1 nM LXA_4 are highly sensitive to PGE_2 and respond to ∼1–2 logs lower PGE_2 concentrations than Mφ not exposed to LXA_4 with a protective response against necrosis (Fig. S1, available at http://www.jem.org/cgi/content/full/jem.20080767/DC1).

PGE_2 suppresses mitochondrial inner membrane perturbation (MPT) and necrosis in Mφ infected with virulent *Mtb*

Virulent H37Rv induce rampant necrosis. In contrast, avirulent H37Ra fail to induce Mφ necrosis (7, 8, 12). The observation

that infection of Mφ with H37Rv induces LXA_4 and inhibits COX2 and prostanoid production, whereas H37Ra infection fails to induce LXA_4 but stimulates COX2 and prostanoid production, led to the hypothesis that H37Rv-induced LXA_4 production may foster Mφ necrosis via inhibition of PGE_2 production. Conversely, H37Ra infection may stimulate PGE_2-mediated inhibition of LXA_4 and prevent Mφ necrosis. By determining the release of the cationic dye $DiCO_6(3)$ from mitochondria, a correlate of Mφ necrosis (41), we first investigated whether prostanoids block induction of H37Rv-induced necrosis. Indeed, increasing micromolar concentrations of PGE_2 significantly decreased cationic dye release from the mitochondria of human Mφ infected with virulent H37Rv (MOI 10) after 24 h (Fig. 3, A–C). These results were dupli-

cated in experiments with mouse Mφ (unpublished data). Addition of exogenous PGE_2 also inhibited necrosis measured by 7-AAD staining of H37Rv-infected Mφ. Specifically, addition of 1 μM PGE_2 to H37Rv-infected Mφ decreased the number of 7-AAD–positive Mφ after 48 h from 29 ± 1 to 17 ± 1% after infection with H37Rv (background 2.2 ± 0.5%; MOI 10:1; P < 0.01; n = 3). Other prostanoids, such as PGD_2, $PGF_{2\alpha}$, PGI_2, and TXA_2, and leukotriene LTB_4, had little or no effect on prevention of necrosis (Fig. 3 C).

We next confirmed the role of PGE_2 in protection against *Mtb* infection-induced necrosis using a loss-of-function approach. In this study, we reasoned that *Mtb*-induced PGE_2 production is a default pathway for the innate immune response, which may be interrupted in H37Rv infection. Thus, infection
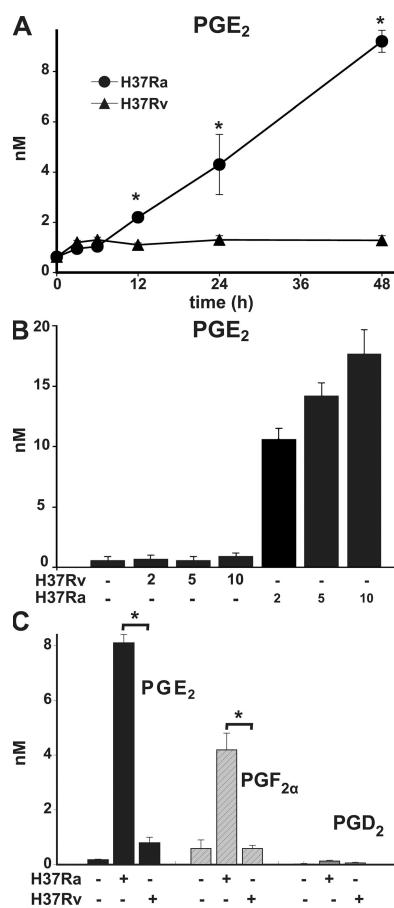
Figure 2. Prostanoid production of Mφ infected with *Mtb*. (A) PGE_2 production of human Mφ 0–48 h after infection with H37Ra and H37Rv (MOI 10:1). Differences in PGE_2 concentrations in supernatants from H37Ra- and H37Rv-infected Mφ are statistically significant (*, P < 0.002; n = 3). (B) PGE_2 production by Mφ infected with H37Ra and H37Rv (MOI 2:1–10:1). The differences in PGE_2 production induced by H37Ra in comparison to H37Rv are statistically significant at all MOIs (*, P < 0.01; n = 3). (C) Quantification of PGE_2, $PGF_{2\alpha}$, and PGD_2 in 48-h supernatants from human Mφ (5 × 10^6 /ml) infected with H37Ra and H37Rv (MOI 10:1; *, P < 0.002; n = 4). Data are presented as means ± SE. In all studies, n represents the number of independent experiments.
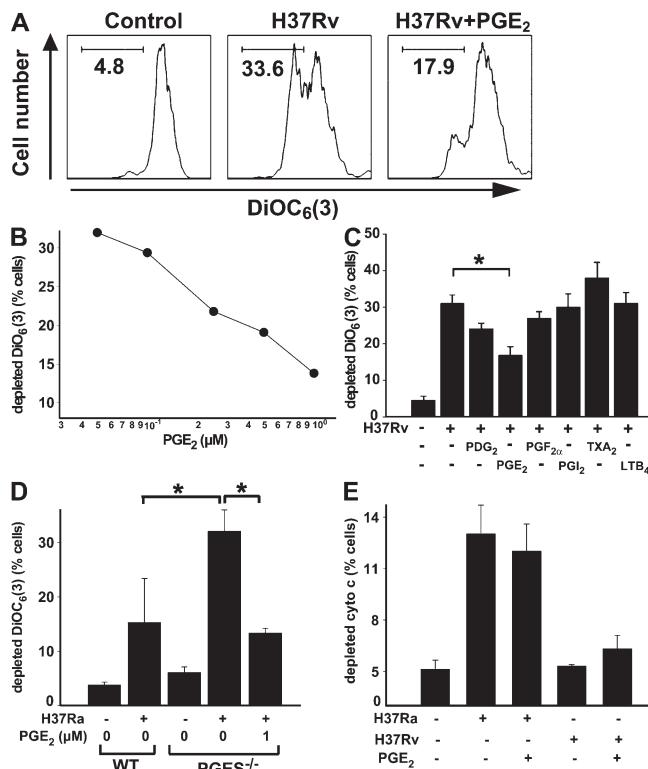
Figure 3. Effect of exogenous prostanoids produced by *Mtb*-infected Mφ on H37Rv–induced mitochondrial cationic dye release. (A) PGE_2 blocks $DiOC_6(3)$ release from mitochondria of human Mφ infected with H37Rv (MOI 5:1; 48 h). A fluorescence-activated cell sorter diagram is shown. (B) Down-regulation of cationic dye release by increasing concentrations of PGE_2 (2–10 μM) is statistically significant at all PGE_2 concentrations (P < 0.01; n = 6). (C) Effect of 1 μM of various prostanoids on H37Rv–induced mitochondrial $DiOC_6(3)$ release of Mφ. Only PGE_2 inhibition of cationic dye release from the mitochondria is statistically significant (*, P < 0.007; n = 3). $PGF_{2\alpha}$ has borderline activity. The concentration of LTB_4 is 0.1 μM. (D) H37Ra (MOI 5:1)-induced $DiOC_6(3)$ release from mitochondria of WT and $PGES^{-/-}$ mouse Mφ infected in the absence and presence of 1 μM PGE_2. At 48 h, cationic dye release from the mitochondria was measured (*, P < 0.006; n = 5). (E) 1 μM PGE_2 does not alter H37Ra- and H37Rv-induced cytochrome *c* release from the mitochondria (not significant; n = 3). Data are presented as means ± SE. In all studies, n represents the number of independent experiments.

of microsomal prostaglandin E synthase (mPGES)$^{-/-}$ Mφ deficient of PGE$_2$ production with H37Ra should mimic the virulent status in H37Rv infection and stimulate necrosis. As anticipated, PGES$^{-/-}$ Mφ (42) are unable to produce PGE$_2$ after infection with avirulent H37Ra and show a concomitant phenotypic switch to susceptibility to necrosis after infection (Fig. 3 D). These results demonstrate that PGES activity inhibits Mtb-induced necrosis. Addition of exogenous PGE$_2$ to H37Ra-infected PGES$^{-/-}$ Mφ restored the avirulent phenotype with striking inhibition of necrosis and confirms that PGE$_2$ is a central mediator in cell death regulation of Mtb-infected Mφ (Fig. 3 D).

To ascertain that induction of human and mouse Mφ necrosis by Mtb is caused by related mechanisms, we determined the amount of necrosis after infection with the same MOIs of H37Ra or H37Rv. The results show that both human and mouse Mφ have a similar necrosis response after infection (Fig. S2, available at http://www.jem.org/cgi/content/full/jem.20080767/DC1).

Defining the existence of distinct mechanisms that regulate necrosis and apoptosis, and having observed a PGE$_2$-dependent modulation in the context of Mtb infection, we next investigated whether PGE$_2$ has a direct role in the regulation of Mφ apoptosis. In this study, we assessed PGE$_2$-stimulated cytochrome c release from the mitochondrial intermembrane space (19), a correlate of apoptosis. Interestingly, we find that PGE$_2$ does not modulate cytochrome c release in H37Ra or H37Rv-infected Mφ (Fig. 3 E), nor does it cause cytochrome c release in absence of infection (not depicted). Thus, PGE$_2$ plays no role in the induction of apoptosis.

Necrosis is positively regulated by LXA$_4$ through inhibition of prostanoid synthesis leading to mitochondrial inner membrane perturbation

In the mouse model of Mtb infection, LXA$_4$ production correlates with reduced resistance against Mtb (38). Our data reveal a relationship between LXA$_4$ production and Mφ necrosis after virulent Mtb infection in vitro. These observations collectively suggest a functional contribution for LXA$_4$ in the induction of necrosis. We reasoned that if LXA$_4$ production is a mechanism by which virulent H37Rv promote necrosis in infected Mφ, addition of LXA$_4$ to Mφ infected with nonvirulent H37Ra should confer a virulent phenotype with regard to Mtb-induced necrosis. Indeed, LXA$_4$ significantly enhanced cationic dye release from the mitochondria, a correlate of necrosis, in H37Ra-infected Mφ (Fig. 4 A, left). Importantly, LXA$_4$ administration in the absence of Mtb infection has no effect on Mφ necrosis (Fig. 4 A, left). Moreover, addition of LXA$_4$ to H37Ra-infected PGES$^{-/-}$ Mφ, which are unable to synthesize PGE$_2$, does not increase cationic dye release from the mitochondria (Fig. 4 A, right). These results suggest that in Mtb-infected Mφ, LXA$_4$ acts by down-regulating PGE$_2$ synthesis to induce necrosis.

To investigate whether induction of necrosis by LXA$_4$ is based on an inhibitory effect of LXA$_4$ on PGE$_2$ synthesis, we determined whether LXA$_4$ blocks synthesis of COX2, thus inhibiting generation of PGE$_2$. Indeed, 10^{-9} M of stable LXA$_4$

analogue added to H37Ra-infected Mφ dramatically inhibited both COX2 protein and PGE$_2$ production induced by H37Ra (Fig. 4 B). Silencing of the 5-LO gene (Fig. 4 C, left) in Mφ infected with the virulent H37Rv inhibited H37Rv-induced LXA$_4$ production (Fig. 4 C, right) and reduced necrosis (Fig. 4 D), demonstrating that 5-LO activity is required for LXA$_4$ production by H37Rv-infected Mφ. Finally, inhibition of LXA$_4$ synthesis in H37Rv-infected Mφ by 5-LO gene silencing led to PGE$_2$ production (Fig. 4 E). These results not only provide additional proof that LXA$_4$ suppresses PGE$_2$ production but demonstrate that the induction of
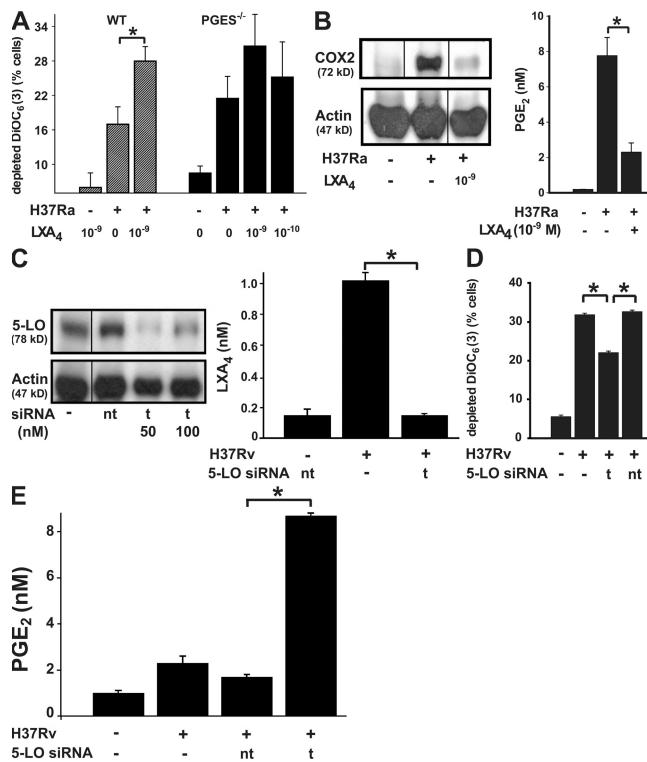
Figure 4. Effect of LXA$_4$ on Mtb–infected Mφ. (A, left) addition of 10^{-9} M LXA$_4$ to H37Ra-infected human Mφ (MOI 10:1) enhances mitochondrial cationic dye release (*, statistically significant difference; n = 3; P = 0.04). (A, right) LXA$_4$ by itself is ineffective. Addition of 10^{-9} and 10^{-10} M LXA$_4$ to PGES$^{-/-}$ mouse Mφ infected with H37Ra (MOI 5:1) does not affect mitochondrial cationic dye release (not significant; n = 3). (B, left) Production of COX2 protein by H37Ra (MOI 10:1)-infected Mφ is inhibited by the addition of 10^{-9} M LXA$_4$. Western analysis of Mφ extracts. The actions of LXA$_4$ were mimicked by its metabolic stable analogue (not depicted). (B, right) PGE$_2$ production by Mφ (*, P < 0.001; n = 3). Black lines indicate that intervening lanes have been spliced out. (C and D) Targeted silencing (t) of the 5-LO gene (C, ∼70% inhibition at t 50) abrogates production of LXA$_4$ by H37Rv-infected Mφ compared with nontargeted (nt) silencing (D, left, 50 nM siRNA; P = 0.001; n = 3) and reduces mitochondrial cationic dye release after H37Rv infection (D, right; nt, nontargeted; P < 0.04; n = 3). Black lines indicate that intervening lanes have been spliced out. (E) Targeted silencing of the 5-LO gene reconstitutes production of PGE$_2$ after infection of Mφ with H37Rv, indicating that block of PGE$_2$ production is caused by the action of LXA$_4$ (P < 0.003; n = 3). Data are presented as means ± SE. In all studies, n represents the number of independent experiments (*, statistically significant).

LXA$_4$ by *Mtb* is a potential mechanism that prevents PGE$_2$ production and leads to cell necrosis.

The prostanoid receptor EP2 is involved in protection of the mitochondrial inner membrane of *Mtb*–infected Mφ by PGE$_2$

The action of PGE$_2$ on the Mφ is mediated by four distinct G protein–coupled E prostanoid (EP) receptors, referred to as EP1, EP2, EP3, and EP4 (43), and mice deficient in the four PGE$_2$ receptors have been generated (44–47). All four receptors are expressed by human Mφ (Fig. 5 A). The EP1 receptor is functionally connected to Gq, a G protein that increases Ca^{2+}$_i$. The EP2 and EP4 receptors activate G proteins that activate adenylate cyclase leading to increased cAMP production. The EP3 receptor inhibits adenylate cyclase via Gi and reduces cAMP levels. To confirm the central role of PGE$_2$ and to more precisely determine its action via specific EP receptors in protection of the mitochondrial inner membrane from MPT, we determined the effect of exogenous PGE$_2$ on cationic dye release in WT Mφ and Mφ from homozygote EP1, EP2, EP3, and EP4$^{-/-}$ mice infected with H37Ra and H37Rv. Mφ from WT, EP1, EP3, and EP4$^{-/-}$ mice responded to increasing exogenous PGE$_2$ concentrations with enhanced inhibition of cationic dye release induced by H37Rv. Cationic dye release from the mitochondria in EP2$^{-/-}$ Mφ infected with H37Rv could not be inhibited even by high concentrations of PGE$_2$, indicating that EP2 is the major PGE$_2$ receptor responsible for inhibition of mitochondrial cationic dye release. Identical results were obtained when the cells were infected with H37Ra (Fig. 5 B).

Stimulation of EP2 and EP4 receptors triggers activation of adenylate cyclase (48). EP2 is associated with activation of protein kinase A (PKA) (49–51). In contrast, signaling through EP4 mainly stimulates phosphatidylinositol-3 kinase (PI3K)–mediated processes (49, 52). To confirm that the inhibition of mitochondrial cationic dye release is modulated by stimulation of EP2, we examined the effect of the specific PKA inhibitor KT5720 (53) on PGE$_2$-dependent inhibition of mitochondrial cationic dye release. We also confirmed lack of involvement of the EP4-stimulated PI3K pathway by testing the effect of the PI3K inhibitor LY294002 on mitochondrial cationic dye release (54). KT5720, at concentrations previously shown to protect cells from apoptosis (10^{-7} M [reference 53]), abrogated the protective effect of PGE$_2$ on Mφ (Fig. 5 C). In agreement with the postulated hypothesis that H37Ra is unable to induce necrosis in infected Mφ because of induction of PGE$_2$ production, addition of KT5720 to H37Ra–infected Mφ significantly augmented Mφ necrosis (Fig. 5 C). In contrast, LY294002 had no effect (Fig. 5 D). KT5720 and LY294002 alone had no effect on mitochondrial cationic dye release induced by H37Rv. These results are consistent with a mechanism wherein EP2 activation of PKA, rather than EP4 activation of PI3K, mediates the protective effect of PGE$_2$ on mitochondria of *Mtb*-infected Mφ.

Pulmonary *Mtb* infection in mice is controlled by PGE$_2$

The findings presented in the previous section indicate that infection with virulent *Mtb* leads to the induction of LXA$_4$ and suppression of PGE$_2$, which results in the necrotic death of infected Mφ. We therefore performed in vitro experiments with Mφ from WT and PGES$^{-/-}$ mice. Fig. 6 A shows that after 4 d of H37Rv infection, the bacterial growth was comparable between WT and PGES$^{-/-}$ Mφ. However, 7 d after infection the bacterial burden was significantly higher in PGES$^{-/-}$ Mφ than in WT Mφ. These data suggested that PGE$_2$ plays a major regulatory role in controlling bacterial growth in Mφ and predicted that an alteration in the balance between PGE$_2$ and LXA$_4$ might change the in vivo outcome of infection. Indeed, 5-LO$^{-/-}$ mice are more
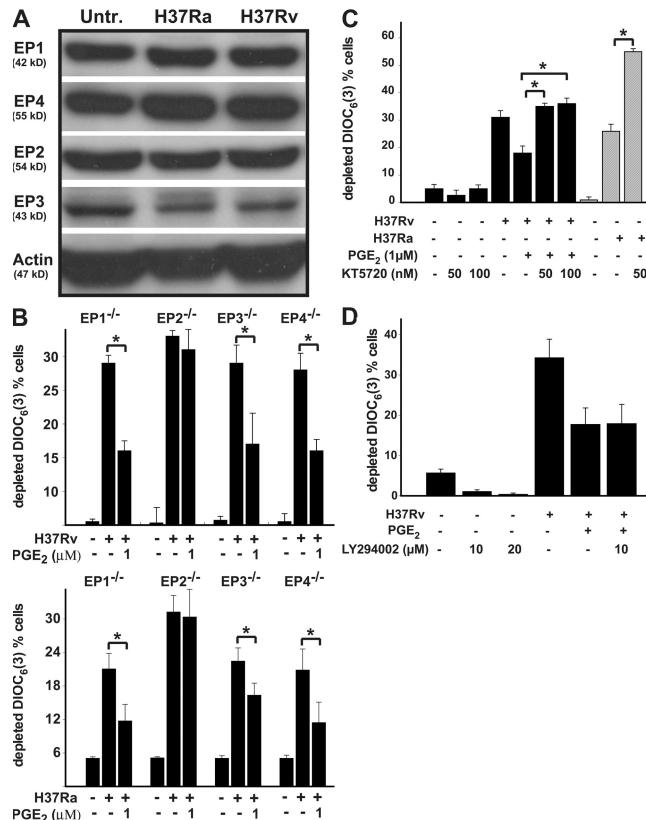

Figure 5. EP2 mediates PGE$_2$–dependent protection against cationic mitochondrial dye release. Data are presented as means ± SE. (A) EP1, EP2, EP3, and EP4 are constitutively expressed in human Mφ. Their expression is not increased by either H37Ra or H37Rv infection. (B) EP2$^{-/-}$ Mφ fail to respond to PGE$_2$ by down-regulating DiCO$_6$(3) release from the mitochondria infected with H37Rv (top) or with H37Ra (bottom), indicating that EP2 mediates the protective function of PGE$_2$. Mφ from EP1, EP3, and EP4 $^{-/-}$ mice were equally responsive to 1 μM PGE$_2$ (*, statistically significant; P < 0.01; n = 5). (C) The cAMP-dependent PKA inhibitor KT5720 abrogates inhibition of mitochondrial cationic dye release by PGE$_2$ (black columns; P < 0.01; n = 3). Addition of KT5720 to H37Ra-infected (MOI 10:1) Mφ enhanced Mφ necrosis (gray columns; *, P < 0.01; n = 3). (D) The PI3K inhibitor LY294002 does not abrogate inhibition of mitochondrial cationic dye release by PGE$_2$ (not significant; n = 3). In all studies, *n* represents the number of independent experiments.

resistant to infection (38). Similarly, we would predict that in the absence of PGES, mice are more susceptible to infection. WT and PGES$^{-/-}$ mice were infected by the aerosol route with 100 virulent *Mtb* per lung. Similar numbers of bacteria were found in the lungs of both WT and PGES$^{-/-}$ mice on day 1 after infection ($n = 4$/group). The bacterial burden in WT and PGES$^{-/-}$ mice was not different 2 wk after infection (unpublished data). However, after 5 wk WT mice controlled the infection more efficiently compared with the PGES$^{-/-}$ mice, whose lungs contained more bacteria (Δ log 10 = 0.97; P = 0.0079; Fig. 6). This difference was not observed in the spleen (unpublished data). To assess whether the balance between PGE$_2$ and LXA$_4$ is changed during the course of a mycobacterial infection in vivo, we next measured the levels of PGE$_2$ and LXA$_4$ in sera from WT mice infected with either virulent Erdmann strain or avirulent H37Ra. As it was observed in vitro, virulent bacteria induced remarkably more LXA$_4$ after 7 d of infection, whereas avirulent H37Ra induced more PGE$_2$. This indicates that PGE$_2$ significantly contributes in vivo to protective responses against mycobacterial infection in the lung.

DISCUSSION
The central finding of this study is that in the local environment of an *Mtb* infection, Mφ infected with virulent *Mtb* preferentially synthesize LXA$_4$ and little, if any, PGE$_2$. In contrast, Mφ infected with avirulent H37Ra produce mainly prostanoids, including PGE$_2$, and only small amounts of LXA$_4$.
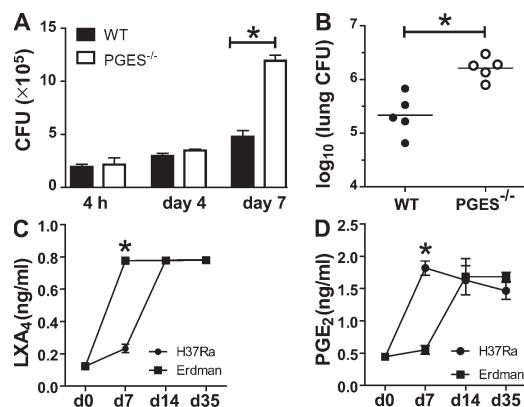
Figure 6. Mycobacterial burden of PGES$^{-/-}$ and WT Mφ in vitro and in vivo. (A) Mycobacterial burden after 4 h (inoculum), 4 d, and 7 d of PGES$^{-/-}$ and WT Mφ in vitro infected with H37Rv (MOI 10:1). The difference in the bacterial burden was significant at 4 and 7 d after infection (*, P < 0.03). (B) 5 wk after aerosol infection, CFUs were determined by plating of homogenized lung tissue as indicated on the ordinate. The difference in mycobacterial burden in the lungs of PGES$^{-/-}$ versus WT mice is statistically significant (*, P = 0.002; five mice per group). (C and D) Induction of LXA$_4$ and PGE$_2$ production during the course of mycobacterial infection. WT mice were infected by aerosol exposure with virulent (Erdmann) or avirulent (H37Ra). LXA$_4$ (C) and PGE$_2$ (D) measured by ELISA in the sera at 7, 14, and 35 d after infection (*, P < 0.01; three mice per time points). These results are representative of two independent experiments. The error bars represent SE.

Our results demonstrate hitherto unappreciated disparate roles for LXA$_4$ and PGE$_2$ in the regulation of induction of host Mφ necrosis, a cell death leading to cytolysis. Mφ infected with virulent *Mtb* that produce LXA$_4$ and reduced amounts of PGE$_2$ undergo necrosis. In contrast, prevention of necrosis and concomitant induction of Mφ apoptosis is associated with increased PGE$_2$ production. Thus, the induction of LXA$_4$ and the resulting inhibition of PGE$_2$ production contribute to the virulence of *Mtb* and enhance its capacity to evade killing by the innate immune system. Indeed, the failure of PGES$^{-/-}$ Mφ to control H37Rv replication in vitro and the observation that PGES$^{-/-}$ mice have a 10-fold higher *Mtb* burden in their lungs compared with WT mice demonstrate the protective effect of PGE$_2$ against virulent *Mtb*. Preferential synthesis of either LXA$_4$ or of prostanoids is a critical branch point for the innate antimycobacterial response of the infected Mφ (Fig. 7).

Lipoxins are best described as potent negative regulators of acute inflammatory processes (55), in part via inhibition of DC mobilization, inhibition of IL12 production (56), and PMN-induced inflammation in vivo. LXA$_4$ activities are multifold and include inhibition of PMN entry to sites of inflammation, reduction of vascular permeability, promotion of monocyte infiltration, and ingestion of apoptotic cells, perhaps including infected Mφ by phagocytes (39). Moreover, lipid mediators that resolve inflammatory events, including LXA$_4$, stimulate phagocytosis of zymosan and of microbial organisms leading to de novo infection of phagocytes (56). The results suggest that the action of LXA$_4$ in reducing prostanoid production as part of the inflammation–resolving program of LXA$_4$ is exploited by *Mtb* in the local environment. Thus, although temporally regulated dampening of the inflammatory response is generally highly beneficial to the host, our studies uncover a novel scenario wherein LXA$_4$-driven reduction of "proinflammatory" PGE$_2$ synthesis functionally acts as an efficient mechanism used by pathogenic *Mtb*. More specifically, LXA$_4$ counteracts the
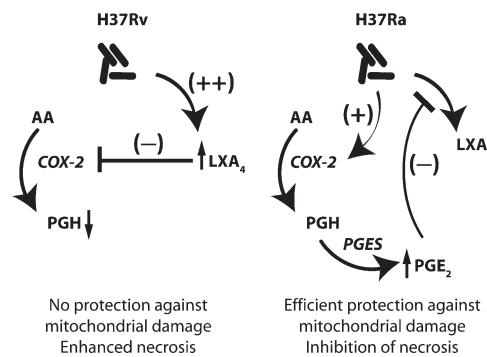

Figure 7. Infection of Mφ with the virulent H37Rv predominantly induces LXA$_4$ production and block of COX2 and PGE$_2$ production, which might lead to necrotic cell lysis and spread of the infection. In contrast, Mφ infected with avirulent H37Ra produce larger amounts of PGE$_2$ which blocks LXA$_4$ production and supports Mφ apoptosis and containment of the *Mtb*. Predominant production of either PGE$_2$ or LXA$_4$ by Mφ infected with H37Ra or H37Rv, respectively, is supported by the fact that PGE$_2$ inhibits LXA$_4$ production and vice versa.

protective effects of PGE$_2$ by inhibiting COX2 expression, thereby causing necrosis in *Mtb*-infected Mφ. Interestingly, LXA$_4$ on its own does not induce necrosis, indicating that the main function of LXA$_4$ is down–regulation of prostanoid production followed by mitochondrial inner membrane destabilization. These results are consistent with studies demonstrating that mycobacterial burden is significantly reduced in 5-LO$^{-/-}$ mice in comparison to WT mice (38) and suggest that LXA$_4$ negatively regulates antimycobacterial defense responses. It should be noted that the concentrations of LXA$_4$ produced are not sufficient to affect inflammatory events in other experimental systems, a feature which is almost certain to be beneficial to the *Mtb* pathogen. Consequently, *Mtb* is able to escape from the necrotic Mφ without adverse effects and is able to infect newly recruited Mφ.

The findings in this paper argue that inhibition of PGE$_2$ comprises a mechanism specific for virulent *Mtb*, a distinctly noninflammatory role for this prostanoid in the regulated response to this pathogen. Prostanoids, including PGE$_2$, are the final product of the PGH synthases COX1 and 2. PGE$_2$ has been extensively studied and is well known for its role in mediating cardinal features of inflammation, including pain, vasodilatation essential for the control of blood flow, and leukocyte diapedesis leading to edema and fever (34). We now show that the prostanoid PGE$_2$ protects against MPT and necrosis of Mφ infected with virulent *Mtb*. Our data are consistent with recently published findings in several other experimental systems that document an inhibitory role of PGE$_2$ in cell death. This mechanism is clearly complex and can be mediated in those studies either by the EP2 receptor (57, 58) or the EP4 receptor (59). Although we definitively confirm the role of PGE$_2$ and more precisely define its mechanistic activity by identifying EP2 as the crucial PGE$_2$ receptor, these findings beg for further dissection of this important signaling pathway leading to increased Mφ defense against *Mtb*.

The mechanisms by which PGE$_2$ stimulates induction of apoptosis of *Mtb*-infected Mφ is not understood. Although PGE$_2$ stimulation of the EP4 receptor triggers activation of PI3K and of Akt (48), blockade of mitochondrial damage by PGE$_2$ critical for prevention of necrosis is mediated through the EP2 receptor. The EP2 subtype couples to G protein α$_s$ and triggers intracellular cAMP formation. cAMP activates the PKA pathway (45), which inhibits death in several cell types (58). PKA activation was found to block cell death by phosphorylation of the proapoptotic protein Bad (49, 50, 54), causing its inactivation, and also increases the expression of Bcl-2 involving the CREB (cAMP responsive element–binding) protein and inhibition of cell death (59). At present, we do not know which of these mechanisms is involved in the mitochondrial inner membrane stabilization by PGE$_2$ and in the inhibition of LXA$_4$ production.

The innate immune system is the first line of defense against invading microbial pathogens and viruses (60). Apoptosis characterized by intact plasma membranes, formation of apoptotic bodies and DNA fragmentation is an important component of the innate immune defense against *Mtb* and is the predominant death modality of the host Mφ infected with attenuated *Mtb* including H37Ra and secA2 mutants (13). Apoptotic bodies are thought to provide a containment vessel for the bacilli as well as an efficient means for pathogen killing (15). Moreover, apoptotic bodies express specific cell surface receptors (61) that promote uptake and subsequent antigen presentation to DC (14). Virulent *Mtb* subvert apoptosis and induce plasma membrane lysis (necrosis), leading to dissipation of the pathogens and spread of the infection.

Thus, the fate of the infected Mφ with regard to cell death modality is a critical determinant in an effective host defense response to *Mtb* infection. Our studies identify a novel mechanism wherein *Mtb* stimulates a pathway involved in the local resolution of inflammation to subvert defense mechanisms against *Mtb*. To our knowledge, this is the first example of a pathway important in the resolution of inflammation that is targeted by a pathogen to counteract the innate immune system. Although it is tempting to advocate therapeutic targets of the lipoxin pathway for *Mtb* infection, further studies are required both to understand the mechanisms by which LXA$_4$ production is activated via virulent *Mtb* and to determine the consequences of blocking the LXA$_4$ production in the course of an infection of Mφ with *Mtb* for the host.

MATERIALS AND METHODS

Materials. LY294002, KT5720, and propidium iodide (PI) were obtained from Sigma-Aldrich. DiOC$_6$(3) (3,3′-dihexyloxycarbocyanine iodide), rhodamine-2 AM, goat anti–mouse IgG$_1$, and anti–mouse COX1 antibodies were obtained from Invitrogen. PGE$_2$, PGF$_{2α}$, PGD$_2$, PGI$_2$, LTB$_4$, TXB$_2$, and LXA$_4$, sheep anti–15-LO antibody, and mouse anti-COX2 antibody were obtained from Cayman Chemical. 15-epi-16-phenoxy-parafluoro-LXA$_4$-methyl ester was a gift from Bayer-Schering Pharma AG. Anti–β-actin mAb was obtained from Thermo Fisher Scientific. Mouse anti–5-LO antibody, mouse IgG$_1$, and mouse anti–cytochrome *c* mAb (7H8.2C12.6H2.B4) were obtained from BD. IMDM, RPMI-1640, Opti-MEM I reduced serum medium, Oligofectamine, Hepes, and DTT were obtained from Invitrogen. Rabbit anti–annexin-1 polyclonal antibody, goat anti–rabbit IgG FITC conjugate, and HRP protein A were obtained from Invitrogen. Anti–phosphatidyl-serine mouse mAb (clone1H6) and rabbit IgG were obtained from Millipore.

Mice. 6–10-wk-old C57BL/6 mice were obtained from Jackson Immuno-Research Laboratories. mPGES-1$^{-/-}$ mice (N5 backcross onto the C57BL/6 background, 45) and EP1 (Ep1$^{-/-}$; reference 47), EP2$^{-/-}$ (48), EP3$^{-/-}$ (47), and EP4$^{-/-}$ mice (51) (n > 10 on C57BL/6 background, provided by B. Koller, University of North Carolina, Chapel Hill, NC) were bred locally. All procedures were approved by the Dana-Farber Cancer Institute Institutional Animal Care and Use Committee.

Bacteria. The virulent *Mtb* strain H37Rv and the attenuated H37Ra (American Type Culture Collection), prepared as described previously (8), were used in the in vitro experiments. The strains were grown in Middlebrook 7H9 broth (BD) with BBL Middlebrook OADC Enrichment (BD) and 0.05% Tween 80 (BD) and resuspended in 7H9 broth at 5 × 10^7 CFU/ml. Aggregation was prevented by sonication for 10 s. The bacteria were allowed to settle for 10 min. Bacteria in Mφ were quantified by lysis of the cells with 0.2% SDS in PBS. After neutralization of SDS with 50% FCS, 100 μl of cell lysates of triplicate cultures were serially diluted 10-fold, plated on 7H10 agar plates (Remel), and colonies were counted after 21 d. Alternatively, the pooled cell lysates were inoculated into triplicate Bactec 12B vials. The number of bacteria was determined with the Bactec model 460 TB system (BD).

Cells and culture. Mononuclear cells from leukopacks of healthy donors or from mouse spleens (7) were plated for FACS analysis at 4×10^5 cells/ml/well in 12-well cluster plates (Corning) and for PI staining and transfection with small interfering RNA (siRNA) at 5×10^5 cells/ml/well in 12-well cluster plates. Human Mφ were cultured for 7 d in IMDM with 10% human AB serum (Gemini Bio-Products) and mouse spleen Mφ for 8–10 d in RPMI 1640 (Invitrogen) with 10% fetal bovine serum (Gemini Bio-Products), 1% Hepes, 1% penicillin/streptomycin, and 0.1% β-mercaptoethanol.

In vitro infection of Mφ. CD11b+ cells were purified from thioglycollate (3%)–elicited peritoneal Mφ harvested from WT and PGES−/− mice by MACS column purification. The purity of the CD11b+ Mφ was 90%. CD11b+ Mφ (10^5/well) were allowed to adhere in a 96-well culture plate for 24 h. Adherent cells were infected with virulent H37Rv (MOI 10: 1) for varying time periods. At different time points, cells were washed extensively with PBS and lysed in H_20 for 5 min, and mycobacterial growth was evaluated by enumeration of the bacilli for 21 d by plating the cell lysates on Middlebrook 7H10 agar plates and incubating at 37°C.

Aerosol infection of mice. C57BL/6 and mPGES-1−/− mice were infected with virulent *Mtb* (Erdman strain) via the aerosol route using a nose-only exposure unit (Intox Products) and received ∼100 CFU/mouse (3, 15, 16). After 5 wk, mice were killed by CO_2 inhalation and the left lung was aseptically removed and individually homogenized in 0.9% NaCl-0.02% Tween 80 with a Mini-Bead Beater 8 (BioSpec Products, Inc.). Viable bacteria were enumerated by plating 10-fold serial dilutions of organ homogenates onto 7H11 agar plates (Remel). Colonies were counted after 3 wk of incubation at 37°C.

LC-MS-MS and ELISA. PGE2, PGF2α, PGD2, and LXA4 concentrations in cell supernatants were determined using ELISA kits (Oxford Biomedical Research) according to the recommendations of the manufacturer. The TXA2 concentration was determined with the TXB2 express EIA kit (Cayman Chemical). 50 µl of culture media from infected Mφ was added to wells in duplicate and absorbance was determined using a microplate reader. The lipid concentration was determined using standard curves. LXA4 and PGE2 identity were confirmed using LC-MS-MS diagnostic ions and their physical properties. For LC-MS-MS, an LCQ ion trap mass spectrometer (Finnigan Corp.) with an electrospray ionization probe was used (62).

Assessment of MPT in Mφ. MPT was assessed in Mφ by measuring retention of the cationic dye DiOC6(3) within the mitochondria (41). Cells were loaded with 3 nM DiOC6(3) in IMDM for 20 min at 37°C. After washing, 20 µg digitonin was added per milliliter and the Mφ were incubated at 37°C for 20 min and fixed with 4% paraformaldehyde for 20 min at room temperature. Cells were dislodged with a rubber policeman, washed with PBS, and resuspended in PBS with 1% BSA. Flow cytometry was performed under FL-1 conditions using a BD FACSort flow cytometer (BD).

Western blotting. After incubation with *Mtb* (MOI 10:1), cells were harvested and lysed with SDS sample buffer (62.5 mM Tris-HCl, pH 6.8, 2% wt/vol SDS, 10% glycerol, 50 mM DTT, 0.01% wt/vol bromophenol blue). The cell lysates were sonicated for 10 s, centrifuged at 10,000 g for 10 min, and dissolved in 15% SDS by using β-actin as a loading control. Mouse anti-COX2 antibody (1:1 dilution), anti–β-actin (1:2,000 dilution; Thermo Fisher Scientific) antibody, mouse anti–5-LO antibody (1:250 dilution; BD) and ovine anti–15-LO antibody (1:250 dilution; Cayman Chemical) were used to detect 5-LO and 15-LO. Rabbit anti-EP1, -EP2, -EP3, and -EP4 receptor antibodies (1:200; Cayman Chemical) were used to detect EP1, EP2, EP3, and EP4 receptor protein.

RT-PCR. Total RNA was extracted as specified in cells-to-cDNA II kit (Ambion). In brief, 5×10^5 mononuclear cells/ml/well in 12-well cluster plates were dislodged and lysed with 100 µl of ice-cold cell lysis II buffer and then 2 µl DNase I was added. Primer sequences used for COX2 were

TTCAAATGAGATTGTGGGAAAATTGCT and AGATCATCTCTG-CCTGAGTATCTT. Primer sequences for GAPDH were ACCACAG-TCCATGCCATCAC and TCCACCACCCTGTTGCTGTA.

PI staining. Adherent mPGES−/− spleen Mφ adherent were stained with 2.5 µg/ml PI in RPMI containing 10% FBS at 4°C for 10 min and washed with ice-cold PBS and H_2O. Dried and mounted coverslips were examined using a fluorescence microscope and photographed with a digital camera (DFC300; Leica).

siRNA transfection. The 5-LO siRNA target sequence (AAATGCCA-CAAGGATTTACCC) targeted against NM_000698 and a scrambled control control siRNA sequence (GCCCTCTATCGAATAAGACAA) designed with siRNA target finder (Ambion) (63) was used. The siRNAs were synthesized from DNA templates with the Silencer siRNA construction kit (Ambion) according to the manufacturer's instructions. Cells were cultured in IMDM with 10% human AB serum, and the medium was changed 1 d before transfection. All siRNAs were used at a final concentration of 50 nM by diluting with Opti-MEM I reduced serum medium. To oligofectamine (1:200 dilution; Invitrogen), fresh IMDM containing 30% human AB serum (Gemini Bio-Products) was added to bring the serum concentration to 10%. After 72 h of transfection at 37°C, the cells were infected with *Mtb*. To examine the effect of siRNA transfection, cells were harvested and analyzed using Northern or Western blotting.

Statistics. Results are expressed as mean ± SEM. The data were analyzed by using Excel Statistical Software (Microsoft) using the Student's t test for normally distributed data with equal variances. CFU were $\log_{10}$ transformed and analyzed using the Mann Whitney nonparametric t test. A p-value <0.05 was considered statistically significant.

Online supplemental material. Fig. S1 shows sensitization of human Mφ with 1 nM LXA4, 1 h before infection with H37Ra (MOI 10:1) to decreasing concentrations of PGE2. Fig. S2 shows FACS analysis of necrotic cells (7-ADD) in human and murine Mφ cultures infected with MOI 10:1 and 20:1 H37Rv and H37Ra for 72 h.

REFERENCES

1. Corbett, E.L., C.J. Watt, N. Walker, B.G. Williams, M.C. Raviglione, and C. Dye. 2003. The growing burden of tuberculosis: global trends, and interactions with the HIV epidemic. *Arch. Intern. Med.* 163: 1009–1021.

2. Dannenberg, A.M., and G.A. Rook. 1994. Pathogenesis of pulmonary tuberculosis: an interplay of tissue-damaging and macrophage-activating immune responses – dual mechanisms that control bacillary multiplication. *In* Tuberculosis. Pathogenesis, Protection and Control. Bloom B R, editor. American Society for Microbiology, Washington DC. 459–484.

3. Leemans, J.C., N.P. Juffermans, S. Florquin, N. van Rooijen, M.J. Verwordeldonk, A. Verbon, S.J.H. van Deventer, T. van der Poll. 2001. Depletion of alveolar macrophages exerts protective effects in pulmonary tuberculosis in mice. *J. Immunol.* 166:4604–4611.

4. Russell, D.G., H.C. Mwandumba, and E.E. Rhoades. 2002. *Mycobacterium* and the coat of many lipids. *J. Cell Biol.* 158:421–426.

5. Sturgill-Koszycki, S., U.E. Schaible, and D.G. Russell. 1996. Mycobacterium-containing phagosomes are accessible to early endosomes and reflect a transitional state in normal phagosome biogenesis. *EMBO J.* 15:6960–6968.

6. Keane, J., M.K. Balcewicz-Sablinska, H.G. Remold, G.L. Chupp, B.B. Meek, M.J. Fenton, and H. Kornfeld. 1997. Infection by *Mycobacterium tuberculosis* promotes human alveolar macrophage apoptosis. *Infect. Immun.* 65:298–304.

7. Park, J.S., M.H. Tamayo, M. Gonzales-Juarrero, I.M. Orme, and D.J. Ordway. 2006. Virulent clinical isolates of *Mycobacterium tuberculosis* grow rapidly and induce cellular necrosis but minimal apoptosis in murine macrophages. *J. Leukoc. Biol.* 79:80–86.

8. Chen, M., H. Gan, and H.G. Remold. 2006. A mechanism of virulence: virulent *Mycobacterium tuberculosis* strain H37Rv, but not attenuated H37Ra, causes significant mitochondrial inner membrane disruption in macrophages leading to necrosis. *J. Immunol.* 176:3707–3716.

9. Kroemer, G., B. Dallaporta, and M. Resche-Rigon. 1998. The mitochondrial death/life regulator in apoptosis and necrosis. *Annu. Rev. Physiol.* 60:619–642.

10. Deshmukh, M., K. Kuida, and E.M. Johnson. 2000. Caspase inhibition extends the commitment to neuronal death beyond cytochrome *c* release to the point of mitochondrial depolarization. *J. Cell Biol.* 150:131–143.

11. Duvall, E., and A.H. Wyllie. 1986. Death and the cell. *Immunol. Today.* 7:115–119.

12. Keane, J., H.G. Remold, and H. Kornfeld. 2000. Virulent *Mycobacterium tuberculosis* strains evade apoptosis of infected alveolar macrophages. *J. Immunol.* 164:2016–2020.

13. Braunstein, M., B.J. Espinose, J. Chan, J.T. Belisle, and W.R. Jacobs. 2003. SecA2 functions in the secretion of superoxide dismutase A and in the virulence of *Mycobacterium tuberculosis*. *Mol. Microbiol.* 48:453–464.

14. Schaible, U.E., F. Winau, P. Sieling, K. Fischer, H.L. Collins, K. Hagens, R.L. Modlin, V. Brinkmann, and S.H. Kaufmann. 2003. Apoptosis facilitates antigen presentation to T lymphocytes through MHC-I and CD1 in tuberculosis. *Nat. Med.* 9:1039–1046.

15. Fratazzi, C., R.D. Arbeit, C. Carini, and H.G. Remold. 1997. Programmed cell death of *Mycobacterium avium* serovar 4 - infected human macrophages prevents the mycobacteria from spreading and induces mycobacterial growth inhibition by freshly added, uninfected macrophages. *J. Immunol.* 158:4320–4327.

16. Molloy, A., P. Laochumroonvorapong, and G. Kaplan. 1994. Apoptosis, but not necrosis, of infected monocytes is coupled with killing of intracellular bacillus Calmette-Guérin. *J. Exp. Med.* 180:1499–1509.

17. Lee, J., H.G. Remold, M.H. Ieung, and H.K. Kornfeld. 2006. Macrophage apoptosis in response to high intracellular burden of *Mycobacterium tuberculosis* is mediated by a novel caspase-independent pathway. *J. Immunol.* 176:4267–4274.

18. Sly, L.M., S.M. Hingley-Wilson, N.E. Reiner, and W.R. McMaster. 2003. Survival of *Mycobacterium tuberculosis* in host macrophages involves resistance to apoptosis dependent upon induction of antiapoptotic Bcl-2 family member Mcl-1. *J. Immunol.* 170:430–437.

19. Green, D.R., and G. Kroemer. 2004. The pathophysiology of mitochondrial cell death. *Science.* 305:626–629.

20. Budd, R.C. 2001. Activation-induced cell death. *Curr. Opin. Immunol.* 13:356–362.

21. Vaux, D.L., and A. Strasser. 1996. The molecular biology of apoptosis. *Proc. Natl. Acad. Sci. USA.* 93:2239–2244.

22. Thornberry, N.A., and Y. Lazebnik. 1998. Caspases: enemies within. *Science.* 281:1312–1316.

23. Rizzuto, R., P. Pinton, D. Ferrari, M. Chami, G. Szabadhai, P.J. Magalhaes, F. DiVirgilio, and T. Pozzan. 2003. Calcium and apoptosis: facts and hypotheses. *Oncogene.* 22:8619–8627.

24. Green, D.R. 2005. Apoptotic pathways: ten minutes to dead. *Cell.* 121:671–674.

25. Frigui, W., D. Bottal, L. Majlessi, M. Monot, E. Josselin, P. Bridin, T. Garnier, B. Gicquel, C. Martin, C. Leclerc, S. T. Cole, and R. Brosch. 2008. Control of *M. tuberculosis* ESAT-6 secretion and specific T cell recognition by PhoP. *PLoS Pathog.* 4:e33.

26. Gan, H., X. He, L. Duan, E. Mirabile-Levens, H. Kornfeld, and H.G. Remold. 2005. Enhancement of antimycobacterial activity of macrophages by stabilization of inner mitochondrial membrane potential. *J. Infect. Dis.* 191:1292–1300.

27. Duan, L., H. Gan, J. Arm, and H.G. Remold. 2001. Cytosolic phospholipase A2 participates with TNF-alpha in the induction of apoptosis of human macrophages infected with *Mycobacterium tuberculosis* H37Ra. *J. Immunol.* 166:7469–7476.

28. Kudo, I., and M. Murakami. 2002. Phosphatase A2 enzymes. *Prostaglandins Other Lipid Mediat.* 68-69:3–58.

29. Wu, Y.L., X.R. Jiang, A.C. Newland, and S.M. Kelsey. 1998. Failure to activate cytosolic phospholipase A2 causes TNF resistance in human leukemic cells. *J. Immunol.* 160:5929–5936.

30. Wissing, D., H. Mouritzen, M. Egeblad, G.G. Poirier, and M. Jaattela. 1997. Involvement of caspase-dependent activation of cytosolic phospholipase A2 in tumor necrosis factor-induced apoptosis. *Proc. Natl. Acad. Sci. USA.* 94:5073–5077.

31. Serhan, C.N. 1997. Lipoxins and novel aspirin-triggered 15-epi-lipoxins (ATL): a jungle of cell-cell interactions or a therapeutic opportunity? *Prostaglandins.* 53:107–137.

32. Godson, C., S. Mitchell, K. Harvey, N.A. Petasis, N. Hogg, and H.R. Brady. 2000. Lipoxins rapidly stimulate nonphlogistic phagocytosis of apoptotic neutrophils by monocyte-derived macrophages. *J. Immunol.* 164:1663–1667.

33. Borgeat, P., and P.H. Naccache. 1990. Biosynthesis and biological activity of leukotriene B4. *Clin. Biochem.* 23:459–468.

34. Rocca, B., and G.A. FitzGerald. 2002. Cyclooxygenases and prostaglandins: shaping up the immune response. *Int. Immunopharmacol.* 2:603–630.

35. Murakami, M., H. Naraba, T. Tanioka, N. Semmyo, Y. Nakatani, F. Kojima, T. Ikeda, M. Fueki, A. Ueno, S. Oh-Ishi, and I. Kudo. 2000. Regulation of prostaglandin E_2 biosynthesis by inducible membrane-associated prostaglandin E_2 synthase that acts in concert with cyclooxygenase-2. *J. Biol. Chem.* 275:32783–32792.

36. Tilley, S.L., T.M. Coffman, and B.H. Coller. 2001. Mixed messages: modulation of inflammation and immune responses by prostaglandins and thromboxanes. *J. Clin. Invest.* 108:15–23.

37. Zamora, R., H. Bult, and A.G. Herman. 1998. The role of prostaglandin E_2 and nitric oxide in cell death in J774 murine macrophages. *Eur. J. Pharmacol.* 349:307–315.

38. Bafica, A., C.A. Scanga, C. Serhan, F. Machado, S. White, A. Sher, and A. Aliberti. 2005. Host control of *Mycobacterium tuberculosis* is regulated by 5-lipoxygenase-dependent lipoxin production. *J. Clin. Invest.* 115:1601–1606.

39. Levy, B.D., G.B. Clish, B. Schmidt, K. Gronert, and C.N. Serhan. 2001. Lipid mediator class switching during acute inflammation: signals in resolution. *Nat. Immunol.* 2:612–619.

40. Clària, J. 2003. Cycolooxygenase-2 biology. *Curr. Pharm. Des.* 9:2177–2190.

41. Zamzami, N., P. Marchetti, M. Castedo, C. Zanin, J.L. Vayssiere, P.X. Petit, and G. Kroemer. 1995. Reduction in mitochondrial potential constitutes an early irreversible step of programmed lymphocyte death in vivo. *J. Exp. Med.* 181:1661–1672.

42. Trebino, C.E., J.L. Stock, C.P. Gibbons, B.M. Naiman, T.S. Wachtmann, J.P. Umland, K. Pandher, J.-M. Lapoite, S. Saha, M.L. Roach, et al. 2003. Impaired inflammatory and pain responses in mice lacking an inducible prostaglandin E synthase. *Proc. Natl. Acad. Sci. USA.* 100:9044–9049.

43. Nataraj, C., D.W. Thomas, S.L. Tilley, M.T. Nguyen, R. Mannon, B.H. Koller, and T.M. Coffman. 2001. Receptors for prostaglandin E (2) that regulate cellular immune responses in the mouse. *J. Clin. Invest.* 108:1229–1235.

44. Stock, J.L., K. Shinjo, J. Burkhardt, M. Roach, K. Taniguchi, T. Ishikawa, H.-S. Kim, P.J. Flannery, T.M. Coffman, J.D. McNeish, and L.P. Audoly. 2001. The prostaglandin E_2 EP1 receptor mediates pain perception and regulates blood pressure. *J. Clin. Invest.* 107:325–331.

45. Tilley, S.L., L.P. Audoly, E.H. Hicks, H.-S. Kim, P. Flannery, T.M. Coffman, and B.H. Koller. 1999. Reproductive failure and reduced blood pressure in mice lacking the EP2 prostaglandin E2 receptor. *J. Clin. Invest.* 103:1539–1545.

46. Fleming, E.F., K. Athirakul, M.I. Oliverio, M. Key, J. Goulet, B.H. Koller, and T.M. Coffman. 1998. Urinary concentrating function in

mice lacking EP3 receptors for prostaglandin E2. *Am. J. Physiol.* 275:F955–F961.

47. Nguyen, M., T. Camenish, J.N. Snouweert, E. Hicks, T.M. Coffman, P.A.W. Anderson, N.N. Malouf, and B.H. Koller. 1997. The prostaglandin receptor EP$_4$ triggers remodeling of the cardiovascular system at birth. *Nature.* 390:78–81.

48. Sugimoto, Y., and S. Narumyia. 2007. Prostaglandin E receptors. *J. Biol. Chem.* 282:11613–11617.

49. Fujino, H., K.A. West, and J.W. Regan. 2002. Phosphorylation of glycogen synthase kinase-3 and stimulation of T-cell factor signaling following activation of EP2 and EP4 prostanoid receptors by prostaglandin E$_2$. *J. Biol. Chem.* 277:2614–2619.

50. Zha, J., H. Harada, E. Yang, J. Jockel, and S.J. Korsmeyer. 1996. Serine phosphorylation of death agonist BAD in response to survival factor results in binding to 14-3-3 not BCL-X(L). *Cell.* 87:619–628.

51. Datta, S.R., A. Katsov, L. Hu, A. Petros, S.W. Fesik, M.B. Yaffe, and M.E. Greenbert. 2000. 14-3-3 proteins and survival kinases cooperate to inactivate BAD by BH3 domain phosphorylation. *Mol. Cell.* 6:41–51.

52. Fujino, H., W. Xu, and J.W. Regan. 2003. Prostaglandin E$_2$ induced functional expression of early growth response factor-1 by EP4, but not EP2, prostanoid receptors via the phosphatidylinositol 3-kinase and extracellular signal–regulated kinases. *J. Biol. Chem.* 278:12151–12156.

53. Simpson, C.S., and B.J. Morris. 1995. Induction of c-fos and zif/268 gene expression in rat striatal neurons, following stimulation of D1-like dopamin receptors, involves protein kinase A and protein kinase C. *Neuroscience.* 68:97–106.

54. Vlahos, C.J., W.F. Matter, R.Y. Hui, and R.F. Brown. 1994. A specific inhibitor of phosphatidylinositol 3-kinase, 2-(4-morpholinyl)-8-phenyl-4H-1-benzopyran-4-one (LY294002). *J. Biol. Chem.* 269:5241–5248.

55. Chiang, N., I.M. Fierro, K. Gronert, and C.N. Serhan. 2000. Activation of lipoxin A$_4$ receptors by aspirin-triggered lipoxins and select peptides evokes ligand-specific responses in inflammation. *J. Exp. Med.* 191:1197–1208.

56. Ariel, A., and C.N. Serhan. 2007. Resolvins and protectins in the termination program of acute inflammation. *Trends Immunol.* 28:176–183.

57. Houchen, C.W., M.A. Sturmoski, S. Anant, R.M. Breyer, and W. Stenson. 2002. Prosurvival and antiapoptotic effects of PGE2 in radiation injury are mediated by EP2 receptor in intestine. *Am. J. Physiol. Gastrointest. Liver Physiol.* 284:G490–G498.

58. George, R.J., M.A. Sturmoski, S. Anant, and C.W. Houchen. 2007. EP4 mediates PGE$_2$ dependent cell survival through the PI3 kinase/AKT pathway. *Prostaglandins Other Lipid Mediat.* 83:112–120.

59. Chen, W., Y.L. Yu, S.F. Lee, Y.J. Chiang, J.R. Chao, J.H. Huang, C.H. Chiong, J. Huang, M.Z. Lai, J.F. Yang-Yen, and J.J. Yen. 2001. CREB is one component of the binding complex of the Ces-2/E2A-HLF binding element and is an integral part of the interleukin-3 survival signal. *Mol. Cell. Biol.* 21:4636–4646.

60. Medzhitov, R., and C.A. Janeway Jr. 1997. Innate immunity: the virtues of a nonclonal system of recognition. *Cell.* 91:295–298.

61. Fadok, V.A., D.L. Bratton, and P.M. Henson. 2001. Phagocyte receptors for apoptotic cells: recognition, uptake, and consequences. *J. Clin. Invest.* 108:957–962.

62. Lu, Y., S. Hong, E. Tjonahen, and C.N. Serhan. 2005. Mediator-lipidomics: databases and search algorithms for PUFA-derived mediators. *J. Lipid Res.* 46:790–802.

63. Elbashir, S.M., J. Harborth, W. Lendeckel, A. Yalcin, K. Weber, and T. Tuschl. 2001. Duplexes of 21-nucleotide RNAs mediate RNA interference in cultured mammalian cells. *Nature.* 411:494–496.